

Synthesis and Properties of Uranium Sulfide Cations. An Evaluation of the Stability of Thiouranyl, $\{S=U=S\}^{2+}$

Cláudia C. L. Pereira,[†] Maria del Carmen Michelini,^{*,‡} Joaquim Marçalo,^{*,†} Yu Gong,[§] and John K. Gibson[§]

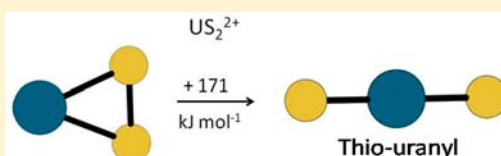
[†]Centro de Ciências e Tecnologias Nucleares, Instituto Superior Técnico, Universidade de Lisboa, 2695-066 Bobadela LRS, Portugal

[‡]Dipartimento di Chimica, Università della Calabria, 87030 Arcavacata di Rende, Italy

[§]Chemical Sciences Division, Lawrence Berkeley National Laboratory (LBNL), Berkeley, California 94720, United States

Supporting Information

ABSTRACT: Atomic uranium cations, U^+ and U^{2+} , reacted with the facile sulfur-atom donor OCS to produce several monopositive and dipositive uranium sulfide species containing up to four sulfur atoms. Sequential abstraction of two sulfur atoms by U^{2+} resulted in US_2^{2+} ; density functional theory computations indicate that the ground-state structure for this species is side-on η^2 - S_2 triangular US_2^{2+} , with the linear thiouranyl isomer, $\{S=U^VI=S\}^{2+}$, some 171 kJ mol^{-1} higher in energy. The result that the linear thiouranyl structure is a local minimum at a moderate energy suggests that it should be feasible to stabilize this moiety in molecular compounds.



INTRODUCTION

The linear dipositive uranyl ion, $\{O=U=O\}^{2+}$, is ubiquitous in condensed-phase actinide chemistry and has accordingly received extensive attention from both the experimental and theoretical perspectives.¹ The synthesis of condensed-phase analogues of uranyl, where oxygen has been replaced by another main-group element, is an ongoing goal. Success in identifying such analogues has included linear diimido complexes, $\{RN=U=NR\}^{2+}$ (R = alkyl or aryl), in which the NR ligand is isoelectronic with oxygen,² a nitrido-substituted analogue with a $\{N\equiv U=O\}^+$ moiety,³ and a $\{R_2C=U=O\}^{2+}$ carbene.⁴ Very recently, Hayton et al. synthesized the chalcogen monosubstituted uranyl analogues $[Cp^*_2Co][U(O)(E)(NR_2)_3]$, where E = S, Se, R = SiMe₃, and $Cp^* = C_5Me_5^-$; the O–U–E bond angles deviate from linearity by only a few degrees.⁵ On the basis of the synthesis of $\{O=U=S\}^{2+}$ and $\{O=U=Se\}^{2+}$ complexes, it is predicted that the synthesis of complexes containing the $\{S=U=S\}^{2+}$ and $\{Se=U=Se\}^{2+}$ moieties should be achievable.⁵

In view of the central role of the UO_2^{2+} moiety, there is particular interest in producing species incorporating bonds between uranium and sulfur, the second short period homologue of oxygen; as emphasized by the recent synthesis of an $[OUS]^{2+}$ complex,⁵ a particular goal is to prepare molecular species incorporating thiouranyl, US_2^{2+} . As an alternative to conventional condensed-phase synthesis, reactions of atomic uranium with atoms and molecules in cryogenic matrices have provided otherwise elusive species and bonding, such as in the linear uranyl-like molecules, NUN^6 and $CUC.^7$ The SUO_2 molecule, prepared and characterized in an inert matrix, exhibits a T-shaped geometry, retaining the robust uranyl moiety and incorporating an equatorial sulfur atom.⁸ The binary US , US_2 , and US_3 molecules have been similarly

matrix-synthesized by the reaction of uranium with sulfur and characterized by IR spectroscopy in conjunction with density functional theory (DFT) calculations.⁹ In contrast to the linear UO_2 molecule,¹⁰ US_2 was found to be highly bent, with an experimental S–U–S bond angle of $118 \pm 5^\circ$ (116° calculated here). Unlike US_2 , the US_3 molecule is similar to its UO_3 analogue, both exhibiting a T-shaped geometry.^{9,11}

Following the pioneering work of Ephritikhine and co-workers,¹² several compounds with U–S bonds have been synthesized, including the recently reported $\{O=U=S\}^{2+}$ complex,⁵ but the $\{S=U=S\}^{2+}$ thiouranyl moiety remains elusive.¹³ Uranium persulfide compounds, in which uranyl is coordinated by bidentate persulfide groups, exhibit analogy with previously reported uranyl peroxide compounds.¹⁴ The compound $Cs_3UP_2S_8$ comprises a terminal U=S bond, which is referred to as a “thiouranyl unit”;¹⁵ however, because this is a uranium(IV) compound and there is no $\{S=U=S\}^{2+}$ moiety, it is not thiouranyl per se. Another complex comprising a terminal U=S bond has recently been reported with a U–S bond distance of 2.48 Å, which is ~ 0.6 Å longer than the corresponding terminal U=O bond distance¹⁶ but only ~ 0.1 Å longer than the U=S distance in the $\{O=U=S\}^{2+}$ complex.⁵ King et al. have recently reported a terminal uranium nitride complex with a $U\equiv N$ triple bond,¹⁷ in which the $U\equiv N$ triple bond length of 1.825 ± 0.015 Å is less than 0.05 Å longer than the U–O bond length in uranyl.^{1b} This and other comparisons reveal a decrease in the efficacy of bonding to uranium down the chalcogen group from oxygen to sulfur, in contrast to a minor decrease across the series from oxygen to nitrogen. Hayton and co-workers have recently reported a complex that

Received: August 8, 2013

Published: November 20, 2013

incorporates a bridging disulfido linkage between two uranium centers.¹⁸

Partly on the basis of the observation that, in contrast to UO_2 , neutral US_2 is bent, Denning has speculated that the uranyl moiety may be restricted to first short-period ligands,^{1b} such as nitrogen in the diimidos.² However, the structural correspondence between the U^{VI} molecules, UO_3 and US_3 , suggests some similarity in bonding and the possibility for a stable thiouranyl moiety, $\{\text{S}=\text{U}=\text{S}\}^{2+}$. A route to such positively charged molecular ions, which may not ultimately be accessible in the condensed phase despite recent accomplishments,⁵ is via reactions of metal ions with neutral molecules in the gas phase. Gas-phase US^+ , US_2^+ , and UOS^+ monocationic ions have been prepared by reactions of U^+ and UO^+ with the sulfur-atom donors CS_2 and COS .¹⁹ More recently, US^+ was produced by the reaction of U^+ with CS_2 , UOS^+ was produced by the reaction of US^+ with CO_2 or OCS , and US_2^+ was produced by the reaction of US^+ with OCS .²⁰ The “bare” uranyl ion, UO_2^{2+} , was previously synthesized in the gas phase by oxidation of U^{2+} to UO_2^{2+} .²¹ It may be similarly possible to synthesize the “bare” thiouranyl ion, $\{\text{S}=\text{U}=\text{S}\}^{2+}$, by the gas-phase reaction of U^{2+} with sulfur-donor molecules. Because the synthesis of a molecular ion with a particular composition and charge does not directly reveal structure and bonding, gas-phase-ion syntheses are generally carried out in conjunction with computational studies of the identified species. In the present work, bare US_2^{2+} , as well as several other uranium sulfide and mixed oxide sulfide ions, were synthesized in the gas phase and characterized by collision-induced dissociation (CID). DFT computations provide structures and energetics for experimentally observed species, with a focus on the nature of US_2^{2+} in the context of the stability of thiouranyl.

METHODS

Experimental Section. Gas-phase reactions were studied by Fourier transform ion-cyclotron resonance mass spectrometry (FTICR-MS) using procedures described in detail recently in a report of our study of actinide monosulfide thermochemistry,²⁰ as well as in the Supporting Information (SI). The $\text{U}^{+/2+}$ ions were produced by laser desorption/ionization of uranium metal and trapped in the ICR cell in which the pressure of the OCS reagent was maintained at $\sim 1 \times 10^{-7}$ Torr. Reactant ions— $\text{U}^{+/2+}$ or sequential product ions—were isolated in the cell, and product ion intensities were monitored as a function of the reaction time. Rate constants, k , were determined from the pseudo-first-order decay of the relative signals of the reactant ions as a function of time at constant neutral reagent pressures. Reaction efficiencies are reported as k/k_{COL} where k_{COL} is the collisional rate constant (see the SI). The typical detection limit for most reactions is $k/k_{\text{COL}} \leq 0.005$; however, the reactions of sulfur-containing ions with OCS , for which interference from oxidation due to the background gases is problematic, have a detection limit of $k/k_{\text{COL}} \leq 0.05$. In CID, ions are excited and undergo energetic collisions with neutral gas atoms, primarily argon, which has been added to the cell; with adequate excitation, ion fragmentation results.

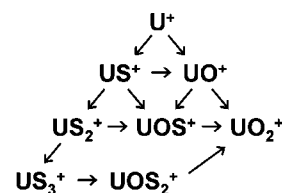
Computational. DFT computations were performed using the *Gaussian 09* (revision B.01) program package.²² Full geometry optimizations and frequency computations were performed using the B3LYP hybrid functional;²³ the Stuttgart–Dresden triple- ζ valence basis sets together with the corresponding effective small-core potential (SDD) were used for uranium²⁴ and the Pople triple- ζ basis sets, 6-311+G(2d), for sulfur.²⁵ The B3LYP functional in combination with the SDD basis sets has previously provided reasonably accurate bond-energy results in actinide-containing systems.^{20,26} All reported energies include the zero-point-energy (ZPE) correction at 0 K. The “ultrafine” option was adopted for

numerical integration. Unrestricted methods were used for all open-shell species. For each of the species studied, different spin multiplicities were tested in order to establish the ground spin state. No significant spin contamination issues were detected; the values of $S(S+1)$ never exceeded the expectation value by more than 1%. Natural bond orbital (NBO) and natural population analysis (NPA) were performed using *NBO 3.1*, as implemented in *Gaussian 09*.²⁷ The nature of the bonding was analyzed by means of the atoms in molecules (AIM)²⁸ approach, using the *AIMAll* program package.²⁹

RESULTS AND DISCUSSION

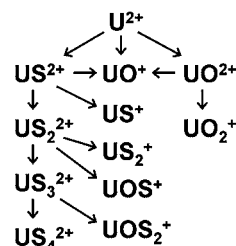
Monopositive and dipositive uranium ions, U^+ and U^{2+} , were reacted with carbonyl sulfide, OCS , in an FTICR-MS spectrometer. Carbonyl sulfide was selected because it is a thermodynamically facile sulfur-atom donor, with the following bond dissociation energies: $D(\text{OC}-\text{S}) = 308 \pm 1 \text{ kJ mol}^{-1}$ and $D(\text{O}-\text{CS}) = 658 \text{ kJ mol}^{-1}$.³⁰ For the case of U^{2+} , an important selection criterion was also the rather high ionization energy of OCS [$\text{IE}(\text{OCS}) = 11.18 \text{ eV}^{30}$], which could disfavor electron-transfer pathways. It was possible to isolate several of the reaction products and study sequential reactions. For several reactions, there were two or three simultaneous pathways. The observed reactions are summarized in Schemes 1 and 2

Scheme 1. Reaction Pathways for the Primary and Sequential Reactions of U^+ with OCS^a



^aAll pathways terminate at UO_2^+ , which is unreactive.

Scheme 2. Reaction Pathways for the Primary and Sequential Reactions of U^{2+} with OCS^a



^aThe monopositive intermediate products react as shown in Scheme 1, all ultimately terminating in UO_2^+ . The two terminal unreactive products for the U^{2+}/OCS reaction sequences are UO_2^+ and US_4^{2+} .

(product branching ratios are in the SI). Because the observed reactions occur under thermal conditions and must be nearly thermoneutral or exothermic, the following U–S bond dissociation energy limits are derived as described in the SI (values are in kilojoules per mole; DFT values are in braces): $436 \leq D(\text{U}^+-\text{S}) \{484\} \leq 560$; $308 \leq D(\text{SU}^+-\text{S}) \{339\} \leq 443$; $308 \leq D(\text{S}_2\text{U}^+-\text{S}) \{313\}$; $D(\text{OU}^+-\text{S}) \leq 528$; $308 \leq D(\text{U}^{2+}-\text{S}) \{347\} \leq 742$; $308 \leq D(\text{SU}^{2+}-\text{S}) \{416\}$; $308 \leq D(\text{S}_2\text{U}^{2+}-\text{S}) \{308\}$; $308 \leq D(\text{S}_3\text{U}^{2+}-\text{S}) \{324\}$. The results for US^+ have been described elsewhere.²⁰ The disulfide results are evaluated with a particular emphasis on the nature of US_2^{2+} in comparison with uranyl, UO_2^{2+} . The results for the trisulfides and tetrasulfides are briefly discussed.

Uranium Disulfides: The Nature of US_2^{2+} . As indicated in Scheme 2, the US_2^{2+} ion was produced by the sequential abstraction of sulfur atoms from two OCS molecules by U^{2+} . The computed structures for the ground state (GS) and the higher-energy thiouranyl isomer of US_2^{2+} are shown in Figure 1, together with the GS structures of US_2 and US_2^+ , for

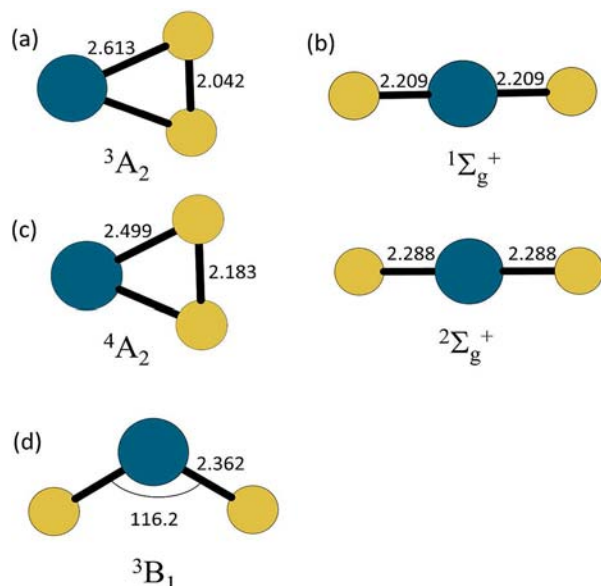


Figure 1. Computed structures of (a) GS US_2^{2+} , (b) US_2^{2+} thiouranyl isomer (171 kJ mol⁻¹ above the GS), (c) GS US_2^+ (the two isomers shown are essentially degenerate in energy, to within 1 kJ mol⁻¹, at the B3LYP/SDD level of theory), and (d) GS US_2 . Bond distances are in angstroms, and angles are in degrees.

comparison. The GS US_2^{2+} isomer has a side-on η^2 - S_2 triangular structure with a S–S distance of 2.042 Å, which is very close to the S–S single-bond distance.³¹ The computed [B3LYP/6-311+G(2d)] S–S bond distance for the free S_2 molecule is 1.923 Å, that for the free $S_2^{\bullet-}$ radical anion is 2.043 Å, essentially the same as that in GS US_2^{2+} , and that for the free S_2^{2-} anion is 2.208 Å. Analysis of the GS US_2^{2+} 3A_2 spin density indicates an α spin density corresponding to three unpaired electrons localized on the uranium atom, and a net spin density of one β electron delocalized on the two sulfur atoms. According to NBO analysis, the $\sigma(U-S)$ bond orbitals are formed from (21% s–60% d–19% f) uranium hybrids and almost (93%) pure sulfur p orbitals. The polarization coefficients (0.902 for sulfur and 0.431 for uranium) indicate that the U–S bond is strongly polarized. The $\sigma(S-S)$ bond is formed from (7% s–91% p–2% d) sulfur hybrids, whereas the $\pi(S-S)$ bond is formed from p pure orbitals and is half-filled. NBO analysis indicates that, in addition to the unpaired α electron located on the $\pi(S-S)$ bond, three other unpaired α electrons are localized on the uranium atom and two β unpaired electrons on each of the sulfur atoms. The charge density, ρ , and $\nabla^2\rho$ at the S–S bond critical points (BCPs) are very close to the corresponding values in the free $S_2^{\bullet-}$ radical anion. A summary of the AIM analysis of the GS structures and some other relevant US_2 , US_2^+ , US_2^{2+} , and UOS^{2+} structures is included as SI (Table S3). For comparison, similar information regarding the GS structures of the corresponding monosulfides and previously reported results for the $UO_2^{+(2+)}$ ions³² are also included in Table S3 in the SI. All U–S bonds are characterized

by a relatively low charge density (ρ) at the U–S BCPs (lower than 0.1 for the triangular structures and between 0.1 and 0.2 for bent and linear structures) and $\nabla^2\rho$ values that are positive and low (between 0.05 and 0.14); the total energy density H (the sum of the kinetic and potential energy densities at the BCP) at the U–S BCPs is in all cases slightly negative. In general, ρ is greater than 0.2 au in covalent (shared) bonds and less than 0.10 au in a closed-shell interaction (for instance, ionic or van der Waals interactions). The Laplacian of the electron density at the BCP, $\nabla^2\rho$, is negative in typical covalent bonding, whereas in interactions characterized by a depletion of density in the region of contact of two atoms, such as ionic, hydrogen-bonding, or van der Waals, it is positive. In strong polar bonding, there is a significant accumulation of electron density between the nuclei, but the Laplacian can be of either sign. More negative values of the total electronic energy density at the BCP, H , reflect greater degrees of covalency. A number of AIM properties of bonding involving uranium and different ligands (i.e., –O, –S, –Cl, –F, –I, –CO, –OH, –NH₂, –CH₃, η^5 -C₅H₅)^{5,32,33} have been reported in the past few years. A comparison of the AIM properties reported by Hayton et al.⁵ for the U–O ($\rho = 0.266$; $H = -0.212$) and U–S ($\rho = 0.123$; $H = -0.054$) bonds of $[Cp^*Co][U(O)(S)(NR_2)_3]$ and the corresponding values for the bare UOS^{2+} linear GS (Table S3 in the SI) computed here indicates that there is a significant decrease of the charge density at both the U–O and U–S BCPs and a significant decrease of the magnitude of H (i.e., a less negative value), as a consequence of the presence of the NR_2 ligands. In uranium monosulfides, the charge density at the BCP increases upon going from US to US^{2+} , in parallel with the shortening of the U–S bond length and the increase of the vibrational frequency (from 448 cm⁻¹ in US to 489 cm⁻¹ in US^{2+}). The linear and bent disulfide isomers show higher BCP charge densities, and more negative H values, than the corresponding triangular isomers. The delocalization indexes show that the average number of electrons delocalized (shared) by the uranium and sulfur atoms is significantly higher in the bent, and even more so, the linear isomers (Table S3 in the SI). The covalency of the U–S bond is, therefore, higher in the thiouranyl isomer; consequently, the relative stability of the isomers is not determined by the higher efficacy of the orbital interactions. In a recent computational study, bond-energy decomposition analysis of US_2 isomers has indicated that the Pauli repulsion reduction that takes place upon going from the linear to the bent structure is a critical contribution that favors the latter, even when orbital interaction favors the linear conformation.³⁴ In early studies, the linear structure of UO_2^{2+} was attributed to the importance of the $5f-2p\pi$ orbital interaction,³⁵ whereas the bent structure of US_2 has been attributed to a greater 6d contribution.³⁶ NPA of the species studied here shows that an important charge rearrangement takes place upon formation of the sulfides and evidence a greater involvement of uranium d orbitals in sulfide bonds compared to similar oxide species (Table S4 in the SI). This is, however, observed in all of the isomers, and the involvement of the 6d orbitals increases upon going from the US_2^{2+} triangular structures to the bent structure (i.e., the structure in which there is not an S–S bond) and even more so in the linear US_2^{2+} structure. The uranium 5f valence population was found to be comparable and in some cases higher in the sulfides than oxides; e.g., in linear US_2^{2+} , the 5f population, 2.86, is slightly greater than that in linear UO_2^{2+} , 2.49 (Table S4 in the SI).

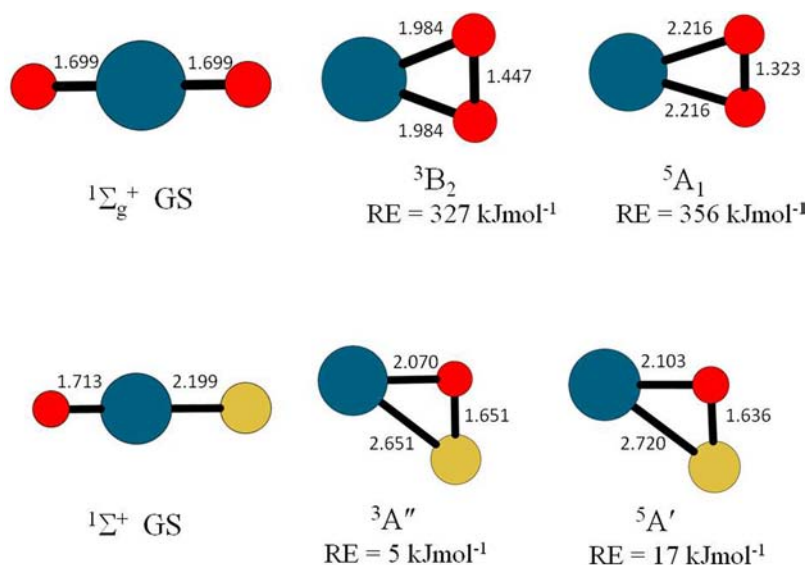


Figure 2. Computed structures of the UO_2^{2+} linear GS and two triangular isomers (top) and of the UOS^{2+} linear GS and two nearly degenerate isomers. RE is the relative energy with respect to the corresponding GS isomer. Bond distances are in angstroms.

A number of triplet and quintet spin triangular isomers very close in energy to the GS 3A_2 —within 18 kJ mol⁻¹ (see Table S5 in the SI)—were located and studied. The presence of several isomers close in energy to the GS US_2^{2+} suggests that multireference ab initio methodologies might be necessary to accurately represent the precise nature of the GS, as has been found to be the case for the GS US_2 .³⁴ However, the linear $\{S=U=S\}^{2+}$ thiouranyl isomer, as well as the bent isomers, are computed to be so much higher in energy than all of the triangular US_2^{2+} electronic structures that it is confidently concluded that the GS has a triangular structure. In particular, the $\{S=U=S\}^{2+}$ thiouranyl isomer is 171 kJ mol⁻¹ higher in energy than the GS. The computed U–S bond distance in linear US_2^{2+} is 2.209 Å, 0.15 Å shorter than that in neutral US_2 , 0.27 Å shorter than the U=S terminal bond length in a molecular complex,¹⁶ and 0.18 Å shorter than that in the $\{O=U=S\}^{2+}$ complex.⁵ The U–S distance in US_2^{2+} is ~0.5 Å longer than the U–O distance in UO_2^{2+} (Figure 2); this elongation is close to the difference between the ionic radii of S^{2-} (1.84 Å; coordination number 6) and O^{2-} (1.40 Å),³⁷ consistent with predominantly ionic bonding.

The computed bond dissociation energies for uranium sulfides are given in Table 1. Cater et al. have reported $D(U-S) = 519 \pm 10$ kJ mol⁻¹ and $D(SU-S) = 515 \pm 20$ kJ

mol⁻¹.³⁸ We have recently reported experimentally derived $D(U-S) = 510 \pm 63$ kJ mol⁻¹.²⁰ The computed value for $D(U-S)$, 536 kJ mol⁻¹, is in good agreement with the experimental values, whereas that computed for $D(SU-S)$, 438 kJ mol⁻¹, is 57 kJ mol⁻¹ below the experimental range. The computed values for $D(SU^+-S)$ and $D(SU^{2+}-S)$ are greater than $D(OC-S)$ such that formation of the disulfide cations is predicted to be thermodynamically favorable, in accordance with the experimental observation of the formation of both US_2^+ and US_2^{2+} .

The results for CID of US_2^{2+} are included in Table 2. The only observed CID channel was charge separation to $US^+ + S^+$.

Table 2. CID Products and Computed Energetics

precursor ion	CID products ^a	computed energies (B3LYP/SDD), kJ mol ⁻¹
US^+	$U^+ + S$	$U^+ + S = 484$
US_2^+	$US^+ + S$	$US^+ + S = 339/U^+ + S_2 = 409$
US_2^{2+}	$U^{2+} + S$	$U^{2+} + S = 347/U^+ + S^+ = 229$
US_2^{2+b}	$US^+ + S^+$	$US^+ + S^+ = 161/U^+ + S_2^+ = 142^b$
US_2^{2+c}	N/A	$US^+ + S^+ = -11/U^+ + S_2^+ = -29^c$
US_3^{2+d}	$US^+ + S_2^+$	$US^+ + S_2^+ = -33/US_2^+ + S^+ = 130$
US_4^{2+d}	$US_2^+ + S_2^+$	$US_2^+ + S_2^+ = -49/US_3^+ + S^+ = 140$

^aOnly one significant CID channel was observed for each species.

^bComputed energies for the US_2^{2+} triangular GS. ^cComputed energies for the high-energy linear thiouranyl isomer, which is assumed to not have been produced in these experiments. ^dGS structures are reported in the SI.

Table 1. Computed Bond Dissociation and Ionization Energies for Uranium Sulfides^a

	$D(S)^b$	$D(S_2)^c$	IE
US	536		614
US^+	484		1269
US^{2+}	347		
US_2	438	561	714
US_2^+	339	409	1193
US_2^{2+}	416	336	
US_3^+	313	238	1198
US_3^{2+}	308	310	
US_4^{2+}	324	218	

^aIn kilojoules per mole. ^bEnergy for $US_n^{q+} \rightarrow US_{n-1}^{q+} + S$. ^cEnergy for $US_n^{q+} \rightarrow US_{n-2}^{q+} + S_2$.

The DFT results indicate that for triangular US_2^{2+} charge separation to $U^+ + S_2^+$ is energetically more favorable, albeit by only 19 kJ mol⁻¹. A possible explanation for observation of the alternative $US^+ + S^+$ product during CID could be related to different charge-separation barriers associated with the different dissociation products. The results in Table 2 reveal that bare linear thiouranyl should be slightly metastable toward dissociation to $US^+ + S^+$ or $U^+ + S_2^+$, by 11 and 29 kJ mol⁻¹, respectively. However, as has been discussed by others, there are inherent and substantial (i.e., at least 100 kJ mol⁻¹) Coulomb barriers to processes that require the separation of doubly charged species into two singly charged species,³⁹ with

the result that bare thiouranyl, if it could be prepared, would likely not spontaneously dissociate, although it could spontaneously rearrange to the GS triangular isomer. Referring to Table 2, a Coulomb barrier to charge separation accounts for the (barrierless) dissociation of US^{2+} to $U^{3+} + S$, rather than to the lower-energy products, $U^+ + S^+$. For the monovalent sulfides, where charge separation is not a possible pathway and there is no Coulomb barrier to separation into a 1+ and a neutral species, the observed dissociations occurred via the computed lowest-energy pathways.

The computed structure of neutral US_2 is very similar to those reported previously.^{9,34} The US_2 molecule has a bent GS 3B_1 structure, with a U–S bond distance of 2.362 Å and a S–U–S angle of 116°. The linear triplet and singlet US_2 structures are higher in energy (at 26 and 60 kJ mol⁻¹, respectively), and the presence of imaginary frequencies indicates that they are not real minima of the US_2 potential energy surface. For US_2^+ , two isomers, linear and triangular, were found to be essentially degenerate in energy (within 1 kJ mol⁻¹) at the level of theory used here (see Figure 1).

A key result of the DFT structures reported here is that both GS US_2^+ and an isomer of US_2^{2+} are linear. Although the GS structure of US_2^{2+} is the triangular isomer (Figure 1a), the higher-energy disulfide is linear, in correspondence to uranyl, and this higher-energy isomer can be considered to be thiouranyl. Scan calculations were performed in order to determine the barrier to interconversion between these two isomers (Figure S3 in the SI). It was found that the barrier involved is ca. 60 kJ mol⁻¹ for both spin states (without ZPE). On the basis of this barrier, thiouranyl is evidently metastable relative to the triangular isomer in the gas phase, but with the imposition of structural constraints, it could be possible to stabilize the linear thiouranyl moiety in the condensed phase. In contrast to the strong U=O bonds in UO_2^{2+} , $D(OU^{2+}-O) = 529 \pm 31$ kJ mol⁻¹,⁴⁰ the U=S computed bond dissociation energy for the linear thiouranyl isomer of US_2^{2+} is only $D(SU^{2+}-S) = 245$ kJ mol⁻¹. The present results suggest that the bonding in thiouranyl is much less effective relative to that in uranyl, which accounts for the GS triangular isomer in which there is S–S bonding.

To further reveal the underlying basis for the structural differences between linear UO_2^{2+} and triangular US_2^{2+} , GS and higher-energy structures of UO_2^{2+} and UOS^{2+} were computed at the same level of theory as that employed for US_2^{2+} , with the results shown in Figure 2. The well-established GS linear uranyl structure is obtained for UO_2^{2+} , with two triangular structures exhibiting O–O bonding higher in energy by more than 300 kJ mol⁻¹. For UOS^{2+} , the GS structure is computed to be linear semithiouranyl, but there are two distorted triangular structures nearly degenerate in energy (within <20 kJ mol⁻¹); these latter structures are stabilized by S–O bonding. While the S–S bonding in the US_2^{2+} triangular GS renders it lower in energy than linear thiouranyl, the S–O bonding in UOS^{2+} renders the linear semithiouranyl and distorted triangular structures nearly degenerate in energy. A key point is that both the $\{S=U=S\}^{2+}$ and $\{S=U=O\}^{2+}$ structures are linear like uranyl.

Thiouranyl is evidently metastable relative to the triangular isomer in the gas phase and exhibits relatively weak U=S bonds, in accordance with the prediction of Denning.^{1b} It should be noted that the recent synthesis of a $\{O=U=S\}^{2+}$ semithiouranyl complex⁵ does not necessarily suggest that thiouranyl is a viable synthetic target. The present results indicate that the GS of gas-phase UOS^{2+} is linear. Only if a

coordination environment could be crafted to circumvent its substantial 171 kJ mol⁻¹ lower stability relative to the triangular structure could the linear thiouranyl moiety be prepared in the condensed phase. It should be noted that the $[(R_2N)_3U](\mu-\eta^2:\eta^2-S_2)$ complex recently reported by Hayton and co-workers,¹⁸ which comprises a triangular US_2 unit capped by another uranium, exhibits a structural unit similar to that identified here for GS US_2^{2+} .

Uranium Polysulfides, US_n^{q+} ($n = 3, 4$; $q = 1, 2$). As shown in Schemes 1 and 2, U^+ sequentially abstracted up to three sulfur atoms from OCS, and U^{2+} abstracted up to four sulfur atoms, to produce the following polysulfides: US_3^+ , US_3^{2+} , and US_4^{2+} . The US_3^+ and US_3^{2+} complexes both react with OCS to produce UOS_2^+ , along with CS_2 or CS_2^+ , respectively; in contrast, US_4^{2+} is inert toward further reaction with OCS. The thermodynamic requirement for a product US_n^{q+} to be produced by sulfur-atom abstraction from OCS by US_{n-1}^{q+} under the thermal experimental conditions is that $D(US_{n-1}^{q+}-S) \geq D(OC-S) = 308 \pm 1$ kJ mol⁻¹ (see Table 1).³⁰

With the exception of US_4^{2+} , the polysulfide ions react with OCS to produce UOS_{n-1}^+ and CS_2 or CS_2^+ (Schemes 1 and 2). As seen in Schemes 1 and 2, the sequential reactions of U^+ and U^{2+} with OCS molecules terminate at unreactive UO_2^+ or US_4^{2+} .

CONCLUSIONS

The U^{2+} ion sequentially abstracts two sulfur atoms from carbonyl sulfide, OCS, to produce the bare gas-phase US_2^{2+} ion. The composition of US_2^{2+} corresponds to thiouranyl, in which the two oxygen atoms in uranyl, UO_2^{2+} , have been substituted by homologous sulfur atoms. DFT computations indicate that the GS structure of US_2^{2+} is a triangular isomer, with the linear thiouranyl structure 171 kJ mol⁻¹ higher in energy. The higher energy of the thiouranyl isomer of US_2^{2+} is consistent with the prediction by Denning that the uranyl-type moiety should be limited to the first short period of elements, including carbon, nitrogen, and oxygen.^{1b}

ASSOCIATED CONTENT

Supporting Information

Experimental details, results of ³⁴S isotopic tracking experiments, reaction rate constants, efficiencies, product distributions, and thermodynamic constraints for the reactions in Schemes 1 and 2, supplemental bond and ionization energies, AIM and NPA analyses of all studied species, relative energies of the US_2^{2+} isomers, potential energy profiles for conversion between the triangular and linear US_2^{2+} isomers (singlet and triplet spin states), GS US_3^{2+} and US_4^{2+} structures, complete ref 22, and mass spectra showing products of the reactions of U^{2+} and US_2^{2+} with OCS. This material is available free of charge via the Internet at <http://pubs.acs.org>.

AUTHOR INFORMATION

Corresponding Authors

*E-mail: mc.michelini@unical.it.

*E-mail: jmarcalo@ctn.ist.utl.pt.

Notes

The authors declare no competing financial interest.

ACKNOWLEDGMENTS

This work was supported by Fundação para a Ciência e a Tecnologia under the Ciência 2007 Programme, by Università della Calabria, and by the U.S. Department of Energy, Office of Basic Energy Sciences, Heavy Element Chemistry, at LBNL under Contract DE-AC02-05CH11231 (Y.G. and J.K.G.). The OCS was a generous gift from Dr. João M. A. Frazão at ISEL, Lisbon, Portugal. This research used resources of the National Energy Research Scientific Computing Center, which is supported by the Office of Science of the U.S. Department of Energy under Contract DE-AC02-05CH11231.

REFERENCES

- (1) (a) Arnold, P. L.; Love, J. B.; Patel, D. *Coord. Chem. Rev.* **2009**, *253* (15–16), 1973–1978. (b) Denning, R. G. *J. Phys. Chem. A* **2007**, *111* (20), 4125–4143. (c) Hayton, T. W.; Fortier, S. *Coord. Chem. Rev.* **2010**, *254* (3–4), 197–214.
- (2) (a) Hayton, T. W.; Boncella, J. M.; Scott, B. L.; Palmer, P. D.; Batista, E. R.; Hay, P. J. *Science* **2005**, *310* (5756), 1941–1943. (b) Boncella, J. M.; Hayton, T. W.; Scott, B. L.; Batista, E. R.; Hay, P. J. *J. Am. Chem. Soc.* **2006**, *128* (32), 10549–10559.
- (3) Fortier, S.; Wu, G.; Hayton, T. W. *J. Am. Chem. Soc.* **2010**, *132* (20), 6888–6889.
- (4) Mills, D. P.; Cooper, O. J.; Tuna, F.; McInnes, E. J. L.; Davies, E. S.; McMaster, J.; Moro, F.; Lewis, W.; Blake, A. J.; Liddle, S. T. *J. Am. Chem. Soc.* **2012**, *134* (24), 10047–10054.
- (5) Brown, J. L.; Fortier, S.; Wu, G.; Kaltsoyannis, N.; Hayton, T. W. *J. Am. Chem. Soc.* **2013**, *135* (14), 5352–5355.
- (6) Hunt, R. D.; Yustein, J. T.; Andrews, L. *J. Chem. Phys.* **1993**, *98* (8), 6070–6074.
- (7) Andrews, L.; Wang, X. F.; Malmqvist, P. A.; Roos, B. O.; Gonçalves, A. P.; Pereira, C. C. L.; Marçalo, J.; Godart, C.; Villeroy, B. *J. Am. Chem. Soc.* **2010**, *132* (24), 8484–8488.
- (8) Andrews, L.; Wang, X. F.; Marsden, C. J. *Inorg. Chem.* **2009**, *48* (14), 6888–6895.
- (9) Liang, B. Y.; Andrews, L.; Ismail, N.; Marsden, C. J. *Inorg. Chem.* **2002**, *41* (11), 2811–2813.
- (10) Gabelnick, S. D.; Reedy, G. T.; Chasanov, M. G. *J. Chem. Phys.* **1973**, *58* (10), 4468–4475.
- (11) Green, D. W.; Reedy, G. T.; Gabelnick, S. D. *J. Chem. Phys.* **1980**, *73* (9), 4207–4216.
- (12) Ventelon, L.; Lescop, C.; Arliguie, T.; Leverd, P. C.; Lance, M.; Nierlich, M.; Ephritikhine, M. *Chem. Commun.* **1999**, *7*, 659–660.
- (13) (a) Yao, J. Y.; Wells, D. M.; Chan, G. H.; Zeng, H. Y.; Ellis, D. E.; Van Duyne, R. P.; Ibers, J. A. *Inorg. Chem.* **2008**, *47* (15), 6873–6879. (b) Oh, G. N.; Ibers, J. A. *Acta Crystallogr., Sect. E* **2011**, *67*, 146–U134. (c) Raw, A. D.; Ibers, J. A. *J. Solid State Chem.* **2012**, *187*, 282–285. (d) Malliakas, C. D.; Yao, J. Y.; Wells, D. M.; Jin, G. B.; Skanthakumar, S.; Choi, E. S.; Balasubramanian, M.; Soderholm, L.; Ellis, D. E.; Kanatzidis, M. G.; Ibers, J. A. *Inorg. Chem.* **2012**, *51* (11), 6153–6163. (e) Bugaris, D. E.; Ibers, J. A. *Inorg. Chem.* **2012**, *51* (1), 661–666. (f) Lam, O. P.; Heinemann, F. W.; Meyer, K. *Chem. Sci.* **2011**, *2* (8), 1538–1547.
- (14) Grant, D. J.; Weng, Z. H.; Jouffret, L. J.; Burns, P. C.; Gagliardi, L. *Inorg. Chem.* **2012**, *51* (14), 7801–7809.
- (15) Neuhausen, C.; Panthofer, M.; Tremel, W. *Z. Anorg. Allg. Chem.* **2013**, *639* (5), 728–732.
- (16) Brown, J. L.; Fortier, S.; Lewis, R. A.; Wu, G.; Hayton, T. W. *J. Am. Chem. Soc.* **2012**, *134*, 15468–15475.
- (17) King, D. M.; Tuna, F.; McInnes, E. J. L.; McMaster, J.; Lewis, W.; Blake, A. J.; Liddle, S. T. *Science* **2012**, *337* (6095), 717–720.
- (18) Brown, J. L.; Wu, G.; Hayton, T. W. *Organometallics* **2013**, *32* (5), 1193–1198.
- (19) Armentrout, P. B.; Beauchamp, J. L. *J. Chem. Phys.* **1980**, *50* (1), 27–36.
- (20) Pereira, C. C. L.; Marsden, C. J.; Marçalo, J.; Gibson, J. K. *Phys. Chem. Chem. Phys.* **2011**, *13* (28), 12940–12958.
- (21) Cornehl, H. H.; Heinemann, C.; Marçalo, J.; de Matos, A. P.; Schwarz, H. *Angew. Chem., Int. Ed. Engl.* **1996**, *35* (8), 891–894.
- (22) Frisch, M. J. *Gaussian 09*, revision B01. See the SI for the full citation.
- (23) (a) Becke, A. D. *J. Chem. Phys.* **1993**, *98* (7), 5648–5652. (b) Lee, C. T.; Yang, W. T.; Parr, R. G. *Phys. Rev. B* **1988**, *37* (2), 785–789.
- (24) (a) Küchle, W.; Dolg, M.; Stoll, H.; Preuss, H. *J. Chem. Phys.* **1994**, *100* (10), 7535–7542. (b) Cao, X. Y.; Dolg, M.; Stoll, H. *J. Chem. Phys.* **2003**, *118* (2), 487–496.
- (25) (a) Krishnan, R.; Binkley, J. S.; Seeger, R.; Pople, J. A. *J. Chem. Phys.* **1980**, *72* (1), 650–654. (b) Blaudeau, J. P.; McGrath, M. P.; Curtiss, L. A.; Radom, L. *J. Chem. Phys.* **1997**, *107* (13), 5016–5021. (c) Clark, T.; Chandrasekhar, J.; Spitznagel, G. W.; Schleyer, P. V. J. *Comput. Chem.* **1983**, *4* (3), 294–301.
- (26) Averkiev, B. B.; Mantina, M.; Valero, R.; Infante, I.; Kovacs, A.; Truhlar, D. G.; Gagliardi, L. *Theor. Chem. Acc.* **2011**, *129* (3–5), 657–666.
- (27) Glendening, E. D.; Reed, A. E.; Carpenter, J. E.; Weinhol, F. NBO, version 3.1.
- (28) Bader, R. F. W. *Atoms in Molecules: A Quantum Theory*; Oxford University Press: Oxford, U.K., 1990.
- (29) Keith, T. A. *AIMAll*, version 13.05.06; TK Gristmill Software: Overland Park, KS, 2013.
- (30) Lias, S. G.; Bartmess, J. E.; Liebman, J. F.; Holmes, J. L.; Levin, R. D.; Mallard, W. G. *J. Phys. Chem. Ref. Data* **1988**, *17*, 1–861.
- (31) Meyer, B. *Chem. Rev.* **1976**, *76* (3), 367–388.
- (32) Michelini, M. C.; Russo, N.; Sicilia, E. *J. Am. Chem. Soc.* **2007**, *129* (14), 4229–4239.
- (33) (a) Petit, L.; Joubert, L.; Maldivi, P.; Adamo, C. *J. Am. Chem. Soc.* **2006**, *128* (7), 2190–2191. (b) Mountain, A. R. E.; Kaltsoyannis, N. *Dalton Trans.* **2013**, *42* (37), 13477–13486. (c) Kaltsoyannis, N. *Inorg. Chem.* **2013**, *52* (7), 3407–3413.
- (34) Andrews, L.; Wang, X. F.; Liang, B. Y.; Ruiperez, F.; Infante, I.; Raw, A. D.; Ibers, J. A. *Eur. J. Inorg. Chem.* **2011**, *28*, 4457–4463.
- (35) Wadt, W. R. *J. Am. Chem. Soc.* **1981**, *103* (20), 6053–6057.
- (36) Tatsumi, K.; Matsubara, I.; Inoue, Y.; Nakamura, A.; Cramer, R. E.; Tagoshi, G. J.; Golen, J. A.; Gilje, J. W. *Inorg. Chem.* **1990**, *29* (24), 4928–4938.
- (37) Lide, D. R. *CRC Handbook of Chemistry and Physics*, 90th ed.; CRC Press: Boca Raton, FL, 2009.
- (38) (a) Cater, E. D.; Rauh, E. G.; Thorn, R. J. *J. Chem. Phys.* **1966**, *44* (8), 3106–3111. (b) Cater, E. D.; Rauh, E. G.; Thorn, R. J. *J. Chem. Phys.* **1968**, *48* (1), 538.
- (39) (a) Spears, K. G.; Fehsenfeld, G. C.; McFarlan, M.; Ferguson, E. *J. Chem. Phys.* **1972**, *56* (6), 2562. (b) Roth, L. M.; Freiser, B. S. *Mass Spectrom. Rev.* **1991**, *10* (4), 303–328. (c) Schröder, D.; Schwarz, H. *J. Phys. Chem. A* **1999**, *103* (37), 7385–7394.
- (40) Marçalo, J.; Gibson, J. K. *J. Phys. Chem. A* **2009**, *113* (45), 12599–12606.